Finite Difference Time Domain Modelling of Hyperthermia Applicators for Cancer Therapy

N M. Pothecary and C J. Railton

Centre for Communications Research,
Faculty of Engineering, University of Bristol,
Bristol BS8 1TR, UK

Abstract

In this contribution an enhanced version of the Finite Difference Time Domain (FDTD) method is used to calculate the field penetration and Specific Absorption Rate (SAR) pattern for a current sheet applicator used in Hyperthermia treatment. The FDTD method uses modified equations to rigorously model three dimensional dielectric boundaries and a non-uniform grid for computational efficiency. Results obtained using the FDTD method are compared with experimental measurements made on phantoms and excellent agreement is obtained.

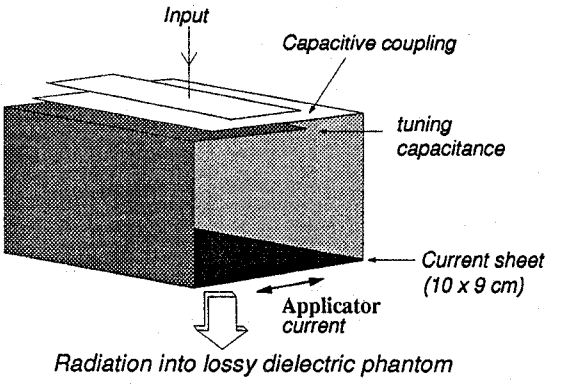

Figure 1: Current sheet applicator for Hyperthermia treatment

1 Introduction

Figure 1 shows the current sheet applicator [1] which can be used for Hyperthermia treatment of cancer. The device can be tuned to a particular frequency and for the tests described in this paper the operating frequency was 86 MHz. A lossy dielectric phantom which consisted of a plastic container filled with saline to a depth of 30 cm was placed against the radiating face of the applicator (10 × 9 cm).

Measurements of the field penetration at 86 MHz into the phantom were made for concentrations in the range 2.5 to $29g/l$. Two different methods were used for the practical measurements, one using a perturbation technique and the other using a dipole [2]. The perturbation method measures power whilst the dipole measures field and the penetration depth is defined as the distance into the dielectric at which the electric field has fallen to e^{-1} of its surface value (for power measurements this corresponds to e^{-2}).

Frequency MHz	Conc. g/l	Permittivity ϵ'	Permittivity ϵ''	σ S/m
86	2.5	78	89	0.42
	5	77	176	0.84
	9	76	311	1.49
	29	70	938	4.49

Table 1: Dielectric properties of phantoms at 86 MHz

Table 1 shows the conductivities and permittivities for saline solutions at 23^0C [2]. These values represent a variation in conductivity of an order of magnitude, thus providing a wide range over which the FDTD method is tested.

2 Enhancements to the basic FDTD algorithm

By modelling the current sheet applicator as the energy source the FDTD method can predict the field distribution in a lossy dielectric phantom. Consequently the field/power penetration and hence the SAR pattern for the phantom can be calculated. It is not necessary to model all the physical parts of the device to obtain accurate results and we have found that it is sufficient to model a U-shaped piece of metal with a current source excited between the open ends. The current source models the physical capacitance which is present in the actual device and its effect is to generate a current which flows over the radiating face of the applicator. The surrounding metal enclosure, tuning capacitance plates and dielectric lid do not need to be included in an FDTD analysis although it is possible to include them. The important parameters are the physical dimensions of the radiating face and the modelling of the excitation source.

However, to obtain accurate values for the penetration depth using the FDTD method the dielectric boundaries must be rigorously modelled. Using too few nodes at a dielectric boundary can cause instability due to the large discretisation error resulting from the rapid change in the normal component of the electric field. For Hyperthermia applicators the applicator/tissue boundary may involve a large change in permittivity from air to high water content tissue and hence the fields will change very rapidly (in these tests the largest permittivity change between air and dielectric was $\epsilon' = 1 \rightarrow \epsilon' = 78$). The node spacing at such a boundary may need to be less than the commonly accepted $\lambda/20$ limit and hence more nodes (and a smaller time-step) will need to be used in a standard FDTD approach [3]. However, by using a non-uniform grid this problem is greatly eased since only in regions of rapid field change are more nodes needed. Away from any boundaries a less dense grid can be used.

The standard FDTD equations for lossy materials have been modified to ensure that dielectric boundaries are rigorously modelled [4]. Continuity of tangential **E** and **H** fields is satisfied for regions involving three dimensional changes in permittivity (Figure 2) thus allowing improved accuracy to be obtained. This approach has the ability to take into account natural features such as the phantom/air boundary as well

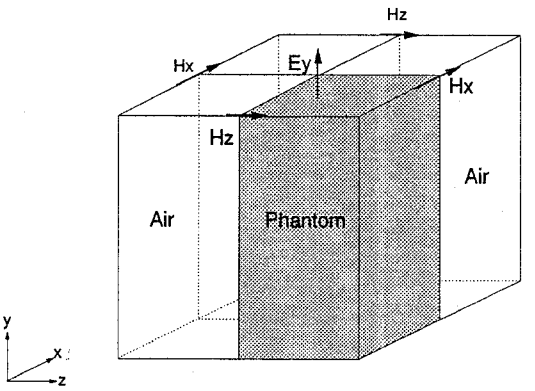

Figure 2: Field components at dielectric boundaries

as the applicator/phantom boundary. This is important since both theoretical calculations and practical measurements indicate that the physical size of the phantom can affect the penetration depth due to reflections from the surrounding phantom/air boundaries.

3 Results

Figure 3 shows both calculated and measured field penetration for various saline concentrations at 86 MHz. For comparison the plane wave values are also shown. The dipole and perturbation methods give very similar results over the range of saline concentrations used and they both show close agreement with the plane wave value at high saline concentrations. The FDTD method agrees with experimental measurements over the whole range of saline concentrations and accurately predicts the "levelling out" of the penetration depth at low saline concentrations. This is a surprising result but it can be explained by the presence of reverse currents in the phantom giving rise to destructive interference and so limiting the penetration depth.

Figure 4 shows a vector plot of the electric field in a plane parallel to and 1cm below the applicator in a $2.5g/l$ phantom dielectric. Null points can clearly be seen on either side of the current sheet and there are regions where the electric field in the dielectric radiates in antiphase to the applicator electric field thus producing the reverse currents. This field pattern calculated by the FDTD method was verified experimen-

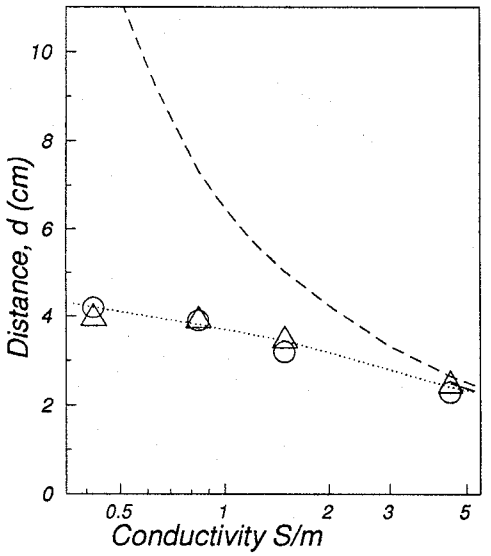

Figure 3: Variation of field penetration, d, with conductivity, σ S/m
○ perturbation, △ dipole, - - plane wave, ··· FDTD

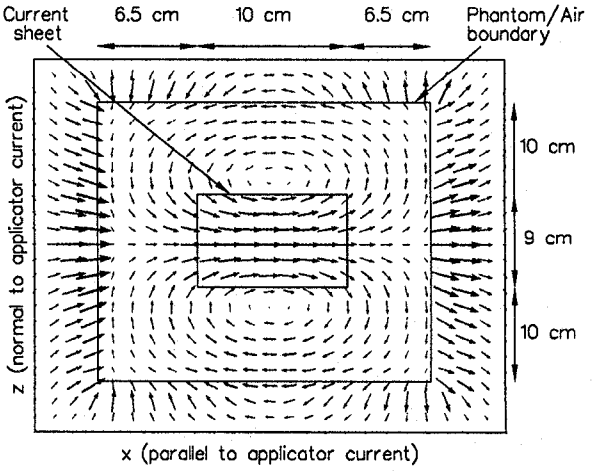

Figure 4: E field vector plot in a plane parallel to and 1cm above the current sheet (86 MHz and 2.5 g/l saline).

tally and good agreement was obtained, including the position of the null points. At high saline concentrations, contributions from these reverse currents are negligible and the penetration depth approaches the plane wave value. The FDTD method can provide a clear pictorial representation of such effects since it accurately models both the displacement and conduction currents which give rise to such phenomena. Figure 4 also shows the surrounding phantom/air boundary and its effect on the electric field pattern. Electric field components normal to the dielectric boundary exhibit a sharp change but components tangential to the boundary are continuous.

The SAR pattern at 86 MHz for the various saline concentrations was also calculated using the FDTD method. Figure 5 shows the SAR pattern for a saline concentration of $2.5g/l$ in a plane parallel to and 1cm below the applicator. There are two positions of zero SAR, one on each side of the applicator, and these correspond to nulls in the electric field pattern (see Figure 4). These null points were also seen in the practical measurements and their position varied only very slightly with saline concentration. For heating applications these null points are important since they represent points of zero energy absorbtion and hence they will not heat in the same manner as surrounding tissue. Indeed, Figure 5 shows the gen-

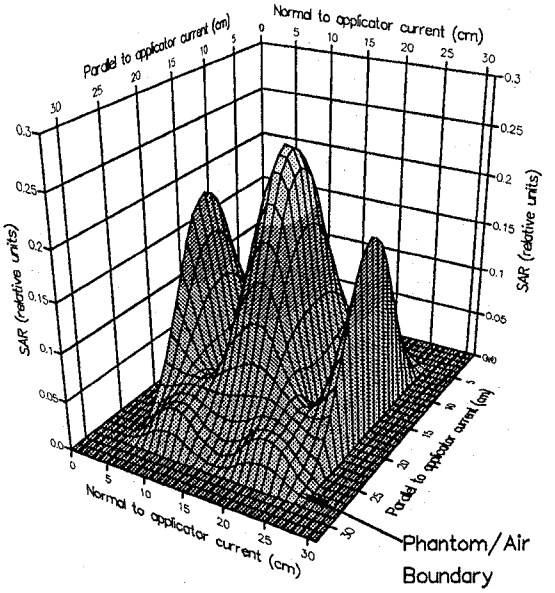

Figure 5: SAR pattern in a plane parallel to and 1cm above the current sheet (86 MHz and 2.5g/l saline)

eral non-uniform SAR pattern that will give rise to a non-uniform heating pattern even when the dielectric and thermal properties are assumed the same for all points.

Figure 5 also clearly shows the phantom/air dielectric boundary which has been modelled by the FDTD method. This corresponds to the practical boundary of air and the dielectric container which holds the saline solution.

Thus any effect of container size on penetration depth and SAR pattern can be modelled using the modified FDTD equations since they take account of just such 3-dimensional boundaries.

4 Conclusion

In this contribution we have shown that an enhanced version of the FDTD algorithm can accurately predict the penetration depth and SAR pattern of practical hyperthermia applicators. Two different experimental techniques have been used and the FDTD method has been shown to be in close agreement with measured data. It is found both experimentally and theoretically that at low phantom conductivities the penetration depth is almost independent of conductivity due to the presence of circulating currents. In addition, the SAR pattern (calculated and measured) shows two null spots whose positions are correctly predicted by the FDTD method and match experimental measurements.

The ability to accurately predict the penetration depth and SAR pattern is essential in Hyperthermia applications as it influences the heating pattern of the electromagnetic applicator. We have shown that it is possible to use the FDTD method for practical problems using a rigorous and computationally efficient algorithm. This is important, since for problems involving complex heterogeneous materials such as biological tissue, the influence of dielectric boundaries should be taken into account.

Acknowledgements

The authors would like to thank Prof J P McGeehan for provision of facilities at the Centre for Communications Research and are grateful to GPT Ltd and SERC UK for financial support.

References

[1] R. H. Johnson, "New types of compact electromagnetic applicator for hyperthermia in the treatment of cancer," *Electronic Letters*, vol. 22, pp. 591–593, May 1986.

[2] R. H. Johnson, M. P. Robinson, A. W. Preece, J. L. Green, N. M. Pothecary, and C. J. Railton, "Effect of frequency and conductivity on field penetration of electromagnetic hyperthermia applicators," *Phys. Med. Bio.*, 1993. Submitted.

[3] P. J. Dimbylow, "FDTD calculations of microwave absorption in the human head," in *8th Annual Review of Progress in Applied Computational Electromagnetics*, 1992.

[4] D. L. Paul, N. M. Pothecary, and C. J. Railton, "Calculation of the dispersive characteristics of open dielectric structures by the Finite-Difference Time-Domain method," *IEEE Trans. on Microwave Theory Tech.*, 1993. Submitted.